AMERICAN SOCIETY FOR MICROBIOLOGY | Applied and Environmental Microbiology®

EVOLUTIONARY AND GENOMIC MICROBIOLOGY

Impact of Cell Surface Molecules on Conjugative Transfer of the Integrative and Conjugative Element ICE*St3* of *Streptococcus thermophilus*

Narimane Dahmane,[a] Emilie Robert,[a] Julien Deschamps,[b] Thierry Meylheuc,[b,c] Christine Delorme,[b] Romain Briandet,[b] Nathalie Leblond-Bourget,[a] Eric Guédon,[d] Sophie Payot[a]

[a]DynAMic, Université de Lorraine, INRA, Vandœuvre-lès-Nancy, France
[b]MICALIS Institute, INRA, AgroParisTech, Université Paris-Saclay, Jouy-en-Josas, France
[c]INRA, Plateforme MIMA2, Jouy-en-Josas, France
[d]STLO, INRA, Agrocampus Ouest, Rennes, France

ABSTRACT Integrative conjugative elements (ICEs) are chromosomal elements that are widely distributed in bacterial genomes, hence contributing to genome plasticity, adaptation, and evolution of bacteria. Conjugation requires a contact between both the donor and the recipient cells and thus likely depends on the composition of the cell surface envelope. In this work, we investigated the impact of different cell surface molecules, including cell surface proteins, wall teichoic acids, lipoteichoic acids, and exopolysaccharides, on the transfer and acquisition of ICE*St3* from *Streptococcus thermophilus*. The transfer of ICE*St3* from wild-type (WT) donor cells to mutated recipient cells increased 5- to 400-fold when recipient cells were affected in lipoproteins, teichoic acids, or exopolysaccharides compared to when the recipient cells were WT. These mutants displayed an increased biofilm-forming ability compared to the WT, suggesting better cell interactions that could contribute to the increase of ICE*St3* acquisition. Microscopic observations of *S. thermophilus* cell surface mutants showed different phenotypes (aggregation in particular) that can also have an impact on conjugation. In contrast, the same mutations did not have the same impact when the donor cells, instead of recipient cells, were mutated. In that case, the transfer frequency of ICE*St3* decreased compared to that with the WT. The same observation was made when both donor and recipient cells were mutated. The dominant effect of mutations in donor cells suggests that modifications of the cell envelope could impair the establishment or activity of the conjugation machinery required for DNA transport.

IMPORTANCE ICEs contribute to horizontal gene transfer of adaptive traits (for example, virulence, antibiotic resistance, or biofilm formation) and play a considerable role in bacterial genome evolution, thus underlining the need of a better understanding of their conjugative mechanism of transfer. While most studies focus on the different functions encoded by ICEs, little is known about the effect of host factors on their conjugative transfer. Using ICE*St3* of *S. thermophilus* as a model, we demonstrated the impact of lipoproteins, teichoic acids, and exopolysaccharides on ICE transfer and acquisition. This opens up new avenues to control gene transfer mediated by ICEs.

KEYWORDS integrative conjugative element, *Streptococcus thermophilus*, biofilm, cell surface molecules, conjugation, exopolysaccharides, gene transfer, lipoteichoic acids, mutant, wall teichoic acids

Horizontal gene transfer (HGT) significantly impacts bacterial evolution by driving genome plasticity. Comparison of the increasingly available prokaryotic genome sequences enables estimation of the intraspecies diversity and reveals a high dynamic

Received 22 September 2017 **Accepted** 13 December 2017

Accepted manuscript posted online 15 December 2017

Citation Dahmane N, Robert E, Deschamps J, Meylheuc T, Delorme C, Briandet R, Leblond-Bourget N, Guédon E, Payot S. 2018. Impact of cell surface molecules on conjugative transfer of the integrative and conjugative element ICE*St3* of *Streptococcus thermophilus*. Appl Environ Microbiol 84:e02109-17. https://doi.org/10.1128/AEM.02109-17.

Editor Maia Kivisaar, University of Tartu

Copyright © 2018 American Society for Microbiology. All Rights Reserved.

Address correspondence to Sophie Payot, sophie.payot-lacroix@inra.fr.

of gene exchanges (1). Conjugation is a mechanism through which the DNA is transferred following the establishment of a cell contact between a donor and a recipient bacterium (2, 3). This mechanism has been found to be the primary contributor to HGT by allowing an effective DNA transfer to a large spectrum of hosts. Mobile genetic elements (MGEs) are essential actors in HGT. Among them, integrative conjugative elements (ICEs), whose sizes range from 18 to 600 kb, are widely distributed in bacterial genomes regardless of the species or any other classification (4–6). ICEs are chromosomal mobile elements that are able to excise from the donor chromosome, transfer by conjugation, and integrate into the recipient chromosome. Like many other MGEs, ICEs owe their evolutionary success in part to the adaptive genes they carry, which can significantly contribute to the competitiveness of their hosts. Hence, ICEs are notably contributing to the spread of antimicrobial resistance (AMR) and the emergence of multidrug-resistant strains, which constitute a serious threat to global public health, as restated recently by the World Health Organization (4, 7). This highlights the necessity of drawing a more comprehensive picture of the conjugative mechanism employed by ICEs. Since conjugation needs a physical contact between the donor and recipient cells, it likely depends on the cell surface composition and on the donor-recipient interactions. Previous studies on ICEs have focused mainly on the mechanisms of transfer and regulation encoded by these elements, whereas the impact of host factors on ICE transfer, including donor and recipient cell surface components, are still poorly described. This has been studied for ICE*Bs1*, an ICE from the Gram-positive bacterium *Bacillus subtilis*, for which the authors reported an impact of the phospholipid biosynthesis pathway on ICE*Bs1* transfer (8, 9). The impact of this pathway has also been tested for Tn*916* by the same group in order to extrapolate the ICE*Bs1* results, demonstrating that some impacts are specific to ICE*Bs1*, whereas others could be generalized to other ICEs (8, 9). A recent study has also showed a role of common polysaccharide antigen, a homopolymer of D-rhamnose attached on lipopolysaccharide, in the initiation of PAPI-1 ICE transfer in *Pseudomonas aeruginosa* (10). In order to provide more information about this topic, we investigated the impact of various cell surface molecules, including surface-exposed proteins, wall teichoic acids (WTA), lipoteichoic acids (LTA), and exopolysaccharides (EPS), on the conjugative transfer of ICE*St3* of *Streptococcus thermophilus*.

ICE*St3* of *S. thermophilus* is a 28-kb element inserted in the 3′ end of the *fda* gene, encoding a 1.6-disphosphate aldolase. It transfers at a frequency of 10^{-6} transconjugants per donor to other *S. thermophilus* strains but also to *Streptococcus pyogenes* and *Enterococcus faecalis* (11). The frequency of transfer of ICE*St3* can be increased 25-fold after exposure of donor cells to mitomycin C treatment (11). ICE*St3* does not encode any known aggregation factor or cell surface-exposed molecule; thus, its transfer depends on successful donor-recipient contacts and likely relies on host factors, as already suggested by a previous study (12).

The Gram-positive bacterium *S. thermophilus* is a clonal species that has recently emerged from a commensal ancestor of the *Streptococcus salivarius* group, which also includes the closely related species *Streptococcus vestibularis* and *Streptococcus salivarius* (13). *S. thermophilus* has evolved mainly by loss of gene functions unnecessary for its adaptation to a narrow and well-defined ecological niche, milk (14–16). This notably includes loss of functions linked with the cell surface composition, making *S. thermophilus* a simple model of cell surface envelope suitable for the purpose of this study.

LPXTG-containing proteins are cell surface proteins covalently linked to the peptidoglycan through the action of sortase enzymes. These proteins are known to fulfill functions mainly linked to the interactions of pathogenic strains with their host (17). Thus, it is not surprising that only rare *S. thermophilus* strains harbor LPXTG proteins at their surface (14).

Lipoproteins (Lpp) are surface proteins covalently linked to the plasma membrane through the sequential action of several enzymes, including the lipoprotein signal peptidase II (LspA) (18).

The bacterial cytoplasmic membrane is a bilayer composed of complex lipids which

vary not only in the length and modifications of their acylated fatty acids but also in the composition of their head groups (19). Some of them are positively charged (e.g., lysylphosphatidylglycerol, synthesized by the MprF protein) (19).

Wall teichoic acids (WTA) are major components of the Gram-positive bacterial envelope (20). Their exposure at the cell surface depends on the action of TagO or its homolog TarO, described in *B. subtilis* and *Staphylococcus aureus* as essential for the initiation of WTA biosynthesis (21, 22). LTA are covalently attached to the plasma membrane through their bond to a glycolipid inserted in the membrane (22). In *S. aureus*, LtaS polymerizes the carbon backbone of LTA, whereas three homologs of LtaS, $LtaS_{BS}$, YfnI, and YqgS, are involved in the biosynthesis of LTA in *B. subtilis* (21, 23, 24). WTA and LTA backbones are maintained with phosphodiester bounds that confer a negative global charge to the whole polymers. For both components, a D-alanylation driven by DltABCD can neutralize the negative charges of the WTA and LTA polymers (21, 25, 26). A *dlt* cluster has been described in *S. thermophilus* LMG 18311 (16).

Exopolysaccharides (EPS) are long chains of polysaccharides that are branched with repeated units of sugar (e.g., glucose, galactose, rhamnose, and derivatives) and are transiently linked to the plasma membrane before their secretion in the neighborhood environment (27, 28). EPS of *S. thermophilus* are well-studied components because of the texture they form, which is useful for the dairy industry. In *S. thermophilus* LMG 18311, a large cluster of genes encodes all the proteins involved in the formation of the repeated sugar units and the export and polymerization of the EPS chain (29–31). The EpsE phosphogalactosyltransferase is essential for EPS production in *S. thermophilus*, since strains lacking this enzyme do not show a detectable amount of EPS (32).

In this study, cell surface mutants of *S. thermophilus* strain LMG 18311 were constructed, characterized (by growth, microscopic observations, and biofilm formation), and used to test their ability to transfer ICE*St3* compared to that of the wild-type (WT) strain. Mating experiments were carried out with either mutated recipients or mutated donors and with both mutated donors and recipients. Whereas some mutations led to an increase, up to 400-fold, of the ICE*St3* transfer frequency, others led to a decrease of the transfer frequency compared to that for the WT. However, none of the tested molecules appeared to be essential for ICE*St3* transfer.

RESULTS

Genes involved in cell surface composition in *S. thermophilus* LMG 18311 and homologs in other bacterial genomes. Eight *S. thermophilus* LMG 18311 mutants were constructed to target cell surface proteins (Δ*lspA* mutant), teichoic acids (Δ*tagO*-like, Δ*yfnI*-like, and Δ*dltA* mutants), lysyl-phosphatidylglycerol biosynthesis (Δ*mprF*-like mutant), and polysaccharide production, including exopolysaccharides (Δ*epsE* and Δ*eps9* Δ*eps10* Δ*eps11* mutants) and rhamnose-glucose polysaccharides (Δ*stu1482* Δ*rgpX2* mutant). Genes encoding some of the targeted functions have already been described (16) or clearly annotated, such as the EPS and *dlt* operons and the *lspA* gene. Identification of genes linked to LTA and WTA functions in *S. thermophilus* required a preliminary *in silico* analysis to detect possible homologs of known coding genes from other bacterial species. Analysis of the available LMG 18311 genome (14) revealed homologs of *B. subtilis* proteins involved in LTA, WTA, and lysyl-phosphatidylglycerol biosynthesis: Stu0163, Stu0636, and Stu1256 were found to be homologous to TagO (33) (41% identity with 86% sequence coverage, E = 2e−69), YfnI (24) (42% identity with 96% sequence coverage, E = 7e−158), and MprF (19) (31% identity with 96% sequence coverage, E = 2e−121), respectively. We searched the LMG 18311 proteome for homologs of the two other proteins, $LtaS_{BS}$ and YqgS, involved in LTA synthesis in *B. subtilis* (24). Stu0636 was the sole protein detected, suggesting that as observed in *S. aureus* (23) and *Listeria monocytogenes* (34), only one LTA synthase is involved in LTA biosynthesis in *S. thermophilus* LMG 18311. Only one LTA synthase was also found in other *S. thermophilus* strains as revealed by *in silico* analyses (e.g., in the TH1435, CNRZ1066, TH1477, and JIM8232 genomes).

Homologs of the 8 genes or clusters of genes selected for mutant construction in *S. thermophilus* LMG18311 were searched in the other available genomes of *S. thermophilus* and the closely related species *S. salivarius*, *S. pyogenes*, and *E. faecalis*. These latter species were chosen since we previously demonstrated transfer of ICE*St3* to a strain of *S. pyogenes* (ATCC 12202) and a strain of *E. faecalis* (JH2-2) (11). Four proteins (Stu0163/TagO, Stu0521/LspA, Stu0636/YfnI, and Stu0761/DltA) appeared to be highly conserved in the 4 species (encoded by 94 to 100% of the strains, with amino acid sequence identities higher than 99%, 91%, 59%, and 45% for the other *S. thermophilus* genomes and the *S. salivarius*, *S. pyogenes*, and *E. faecalis* genomes, respectively). Stu1256/MprF was found in all the genomes of *S. thermophilus* (99 to 100% identity) and *S. salivarius* (88 to 92% identity) and in 98% of the strains of *E. faecalis* (40 to 42% identity). Stu1108/EpsE (with at least 50% of query cover and more than 40% identity with LMG 18311) was found in the majority of the genomes of *S. thermophilus* (>78% with >94% identity) and in all *S. salivarius* genomes (with 76 to 97% identity). In contrast, the rhamnose synthesis cluster was found in only one-third of the *S. thermophilus* and *S. salivarius* genomes, and sequence conservation was lower (from 62% to 98% amino acid identity). The *stu1097 stu1098 stu1099* Eps synthesis cluster was found to be specific to LMG 18311, since no homolog (with >40% amino acid identity) was found in the other genomes examined.

Characterization of cell surface mutants. (i) Growth properties of mutants. None of the cell surface mutants displayed drastic growth defects compared to the WT during growth in M17 broth complemented with 0.5% lactose. We noted, however, that the Δ*yfnI*-like and Δ*stu1482* Δ*rgpX2* mutants showed a higher generation time (46 ± 1 min and 62 ± 1 min, respectively) than the WT (30 ± 1 min), while the Δ*lspA*, Δ*tagO*-like, Δ*epsE*, and Δ*eps9* Δ*eps10* Δ*eps11* mutants displayed generation times (28 ± 1 min, 32 ± 1 min, 32 ± 1 min, and 32 ± 1 min, respectively) close to those of the WT.

(ii) Morphological characteristics of mutants. The LMG 18311 WT strain and cell surface mutants were observed with scanning electron microscopy (SEM) and transmission electron microscopy (TEM) in order to characterize the cell, surface, and chain morphology. LMG 18311 WT cells displayed a homogenous size and were assembled in typical ovococci chains, with septa formed in successive parallel planes perpendicular to the chain axis (Fig. 1). In WT cells, exopolysaccharides appeared as disseminated white spots at the cell surface when using SEM (Fig. 1A, upper panels, black arrows) and as amorphous structures surrounding cells when using TEM (Fig. 1A, lower panels, black arrows). All the mutants except the Δ*epsE* and Δ*eps9* Δ*eps10* Δ*eps11* mutants shared these characteristics (Fig. 1A), thus confirming that the latter mutants lack exopolysaccharides. It also appeared that wall teichoic and lipoteichoic acid mutants displayed an aberrant pattern of septation and cell separation during division (Fig. 1B). Furthermore, two mutants (the Δ*tagO*-like and Δ*dltA* mutants) formed aggregates compared to the WT (see Fig. S3 in the supplemental material for the Δ*tagO*-like mutant).

Finally, the two mutants linked to EPS biosynthesis (Δ*epsE* and Δ*eps9* Δ*eps10* Δ*eps11* mutants) exhibited a distinguishable phenotype of sedimentation in liquid culture compared to the WT (Fig. 2). This phenotype was likely linked to the number of cells per chain of these mutants, which was greater than in the WT, as observed by phase-contrast microscopy (Fig. 2).

(iii) Cell surface charge of mutants. In order to characterize the impact of mutations on the global charge of the cell surface envelope, the zeta potential of mutants was compared to that of the WT at various pHs. At very acidic pH (around pH 2), the zeta potentials of the Δ*epsE* and Δ*eps9* Δ*eps10* Δ*eps11* mutants differed from those of the WT and other mutants with a more positively charged zeta potential (close to 10 mV compared to less than 5 mV) (see Fig. S1 in the supplemental material). The zeta potentials of the WT and mutants were negative at the three tested pHs, pH 5, 7, and 9. At the two latter pHs, the Δ*epsE* and Δ*eps9* Δ*eps10* Δ*eps11* mutants displayed a more negative zeta potential than the WT and other mutants (Fig. S1).

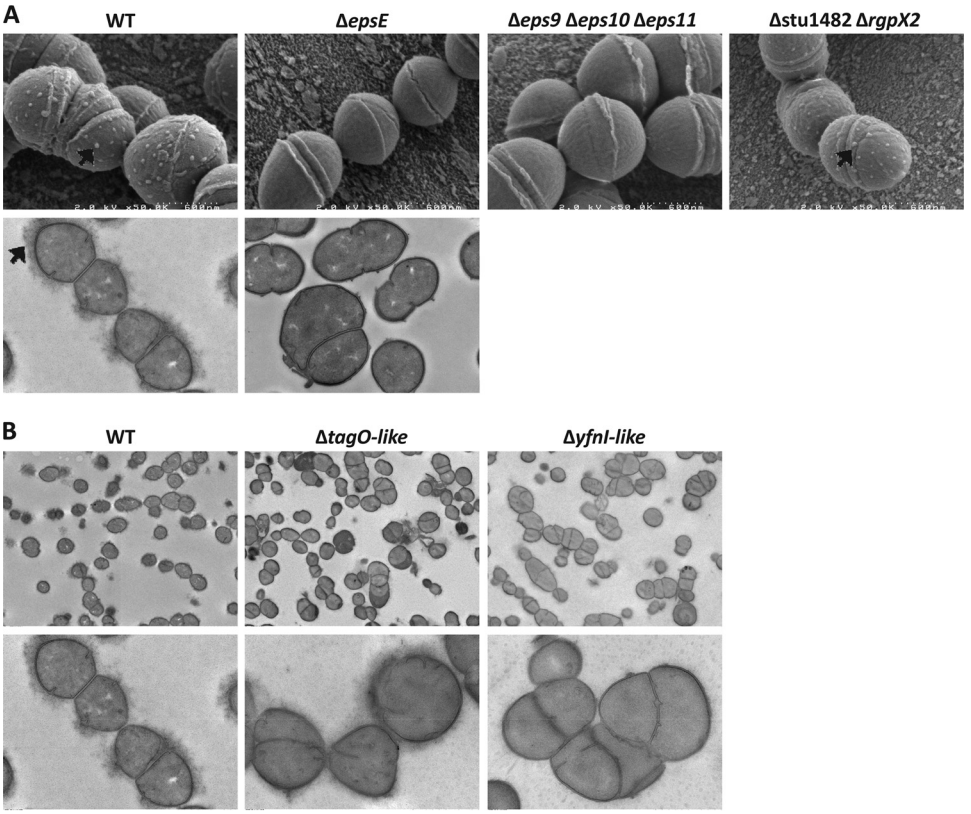

FIG 1 Scanning electron microscopy (SEM) and transmission electron microscopy (TEM) observations of WT LMG 18311 and mutants. (A) SEM observations (original magnification, ×50,000) (upper panels) and TEM observations (original magnification, ×10,000) (lower panels) for the indicated strains. Black arrows indicate EPS. (B) TEM observations (original magnification, ×2,500 [upper panels] and ×10,000 [lower panels]) for the *epsE* mutant compared to the WT.

(iv) Biofilm-forming abilities of mutants. Biofilm formation was evaluated after different time lapses (2 h, 6 h, and 15 h) and measured two times: before and after rinsing the 96-well polystyrene plates to test the robustness of the formed biofilms. The quantitative comparison of biofilm biovolumes showed diversity in biofilm formation compared to that of the WT. Before rinsing, the Δ*yfnI*-like mutant showed a significant higher biofilm biovolume than the WT after 6 h of growth (Fig. 3A). After 15 h of growth, all mutants except the Δ*mprF*-like mutant showed at least a 2-fold higher biofilm biovolume than the WT (Fig. 3A). After rinsing of the well plates, the Δ*lspA* mutant stood out from the WT and other mutants as shown by the robustness of its biofilm structure, with a 7-fold higher biofilm biovolume after 15 h of growth than the

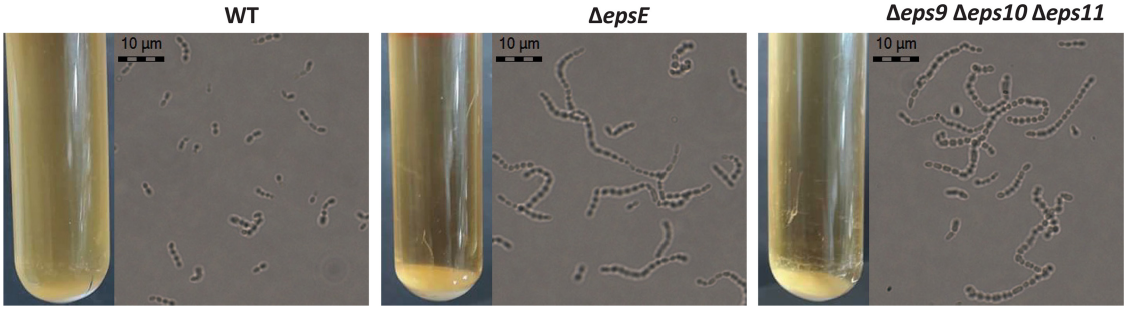

FIG 2 Sedimentation and chain length of WT LMG 18311 and EPS mutants. The picture shows standing LM17 cultures and phase-contrast microscopy of the LMG 18311 WT, Δ*epsE*, and Δ*eps9* Δ*eps10* Δ*eps11* strains. Photographs were taken after 8 h of growth at 42°C in LM17 medium, corresponding to the conditions where sedimentation is visible. Original magnification, ×400.

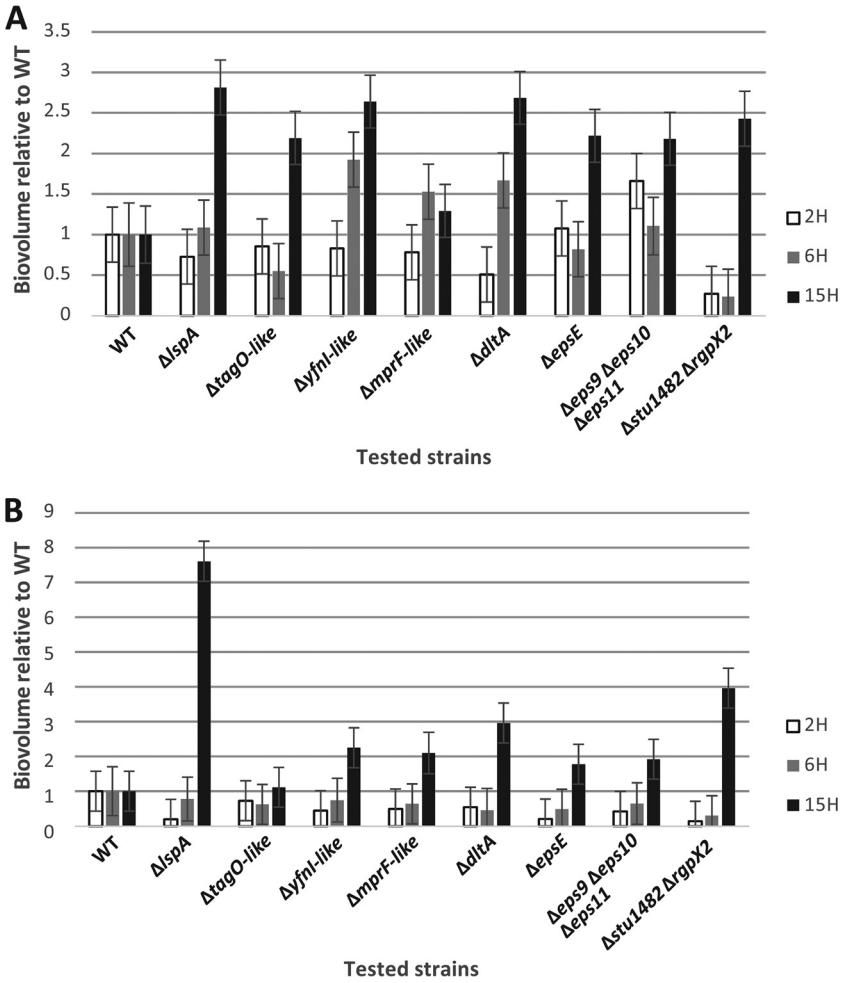

FIG 3 Biofilm biovolumes of LMG 18311 mutants relative to the WT after 2, 6, and 15 h of growth, before (A) and after (B) rinsing of the polystyrene microplates. Error bars show standard errors of the means.

WT (Fig. 3B). Two other mutants (the Δ*dltA*, and Δ*stu1482* Δ*rgpX2* mutants) also displayed a robust biofilm structure compared to that of the WT after 15 h of growth (Fig. 3B).

Conjugative transfer of ICE*St3* using mutated recipients. To test whether the cell surface properties impact the transfer of ICE*St3*, mating experiments were first carried out using mutated recipient cells as detailed in Table 1.

(i) Mating experiments using recipient cells affected in protein exposure (Δ*srtA* and Δ*lspA* mutants). Strain LMG 18311 harbors a truncated *srtA* gene and three pseudogenes of LPXTG proteins. An efficient transfer was observed using this strain as either the donor or recipient in conjugation experiments. This indicates that LPXTG proteins are not essential for transfer and acquisition of ICE*St3*. Experiments were also carried out using the LMD-9 strain of *S. thermophilus*, which harbors a functional sortase A protein and has three LPXTG proteins exposed at its surface. The LMD-9 Δ*srtA* mutant is a strain with a sortase A gene that was interrupted to inhibit the synthesis of SrtA (32). No significant difference in ICE*St3* acquisition was observed when using WT LMG 18311(ICE*St3*) Cm^r as a donor and LMD-9 Δ*srtA* Ery^r or LMD-9(pMG36e) Ery^r as a recipient (see Fig. S2 in the supplemental material).

In contrast, an *lspA* mutation in LMG 18311 led to a 100-fold increase of ICE*St3* acquisition compared to that for a WT recipient strain (i.e., LMG 18311 Ery^r) ($P < 0.01$, *t* test) (Fig. 4A).

(ii) Mating experiments using recipient cells affected in WTA (Δ*tagO*-like mutant) and LTA (Δ*yfnI*-like mutant) exposure. The Δ*tagO*-like and Δ*yfnI*-like

TABLE 1 Bacterial strains and plasmids used in this study

Strain or plasmid	Relevant phenotype[a]	Source or reference
Strains		
LMG 18311	Wild-type strain	
LMG 18311(ICE*St3*)	LMG 18311 carrying ICE*St3* tagged with a chloramphenicol resistance cassette; Cm^r	11
LMG 18311(ICE*St3* GFP)	LMG 18311 carrying ICE*St3* tagged with a chloramphenicol resistance cassette and with a GFP gene under the control of the pLDH promoter of *S. thermophilus* LMG 18311; Cm^r	This work
LMG 18311 Ery^r	LMG 18311 carrying an erythromycin resistance cassette in its chromosome between *stu0627* and *stu0629* genes; Ery^r	This work
LMG 18311 Spc^r	LMG 18311 carrying a spectinomycin resistance cassette in its chromosome between *stu0627* and *stu0629* genes; Spc^r	This work
LMD-9(pMG36e)	LMD-9 carrying the pMG36e plasmid conferring erythromycin resistance; Ery^r	This work
Mutated recipient cells for mating with WT donor cells		
LMG 18311 Δ*lspA*	LMG 18311 with *lspA* (*stu0521*) gene deleted by insertion of an erythromycin cassette; Ery^r	This work
LMG 18311 Δ*tagO*-like	LMG 18311 with *tagO*-like (*stu0163*) gene deleted by insertion of an erythromycin cassette; Ery^r	This work
LMG 18311 Δ*dltA*-like	LMG 18311 with *dltA* (*stu0761*) gene deleted by insertion of an erythromycin cassette; Ery^r	This work
LMG 18311 Δ*yfnI*-like	LMG 18311 with *yfnI*-like (*stu0636*) gene deleted by insertion of an erythromycin cassette; Ery^r	This work
LMG 18311 Δ*mprF*-like	LMG 18311 with *mprF*-like (*stu1256*) gene deleted by insertion of an erythromycin cassette; Ery^r	This work
LMG 18311 Δ*epsE*	LMG 18311 with *epsE* (*stu1108*) gene deleted by insertion of an erythromycin cassette; Ery^r	This work
LMG 18311 Δ*eps9* Δ*eps10* Δ*eps11*	LMG 18311 with *eps9* to *eps11* (*stu1097* to *stu1099*) genes deleted by insertion of an erythromycin cassette; Ery^r	This work
LMG 18311 Δ*stu1482* Δ*rgpX2*	LMG 18311 with *stu1482* and *rgpX2* (*stu1482* and *stu1473*) genes deleted by insertion of an erythromycin cassette; Ery^r	This work
LMD-9 Δ*srtA*	LMD-9 with *srtA* gene deleted by insertion of an erythromycin cassette; Ery^r	43
Mutated donor cells for mating with WT recipient cells		
LMG 18311(ICE*St3*) Δ*lspA*	LMG 18311 Δ*lspA* carrying ICE*St3*; Ery^r Cm^r	This work
LMG 18311(ICE*St3*) Δ*tagO*-like	LMG 18311 Δ*tagO*-like carrying ICE*St3*; Ery^r Cm^r	This work
LMG 18311(ICE*St3*) Δ*dltA*-like	LMG 18311 Δ*dltA*-like carrying ICE*St3*; Ery^r Cm^r	This work
LMG 18311(ICE*St3*) Δ*yfnI*-like	LMG 18311 Δ*yfnI*-like carrying ICE*St3*; Ery^r Cm^r	This work
LMG 18311(ICE*St3*) Δ*mprF*-like	LMG 18311 Δ*mprF*-like carrying ICE*St3*; Ery^r Cm^r	This work
LMG 18311(ICE*St3*) Δ*epsE*	LMG 18311 Δ*epsE* carrying ICE*St3*; Ery^r Cm^r	This work
LMG 18311(ICE*St3*) Δ*eps9* Δ*eps10* Δ*eps11*	LMG 18311 Δ*eps9* Δ*eps10* Δ*eps11* carrying ICE*St3*; Ery^r Cm^r	This work
Mutated recipient cells used in mutant/mutant experiments		
LMG 18311 Δ*lspA*	LMG 18311 Δ*lspA* with spectinomycin resistance cassette; Ery^r Spc^r	This work
LMG 18311 Δ*tagO*-like	LMG 18311 Δ*tagO*-like with spectinomycin resistance cassette; Ery^r Spc^r	This work
LMG 18311 Δ*yfnI*-like	LMG 18311 Δ*yfnI*-like with spectinomycin resistance cassette; Ery^r Spc^r	This work
LMG 18311 Δ*epsE*	LMG 18311 Δ*epsE* with spectinomycin resistance cassette; Ery^r Spc^r	This work
Plasmids		
pMG36e	3.4 kb, replication origin from pWV01; Ery^r	44
pG$^+$host9	4.6 kb, thermosensitive derivative of pWV01; Ery^r	45
pSL1180 spec lox	4.5 kb, derivative of pBR322; Spc^r	This work
pSET4s	4.5 kb, thermosensitive derivative of pWV01; Spc^r	46
pOri23	5.8 kb, ColE1 replication origin; Ery^r	47
pOri23-pLDH	pOri23 with the promoter of the L-lactate dehydrogenase gene (*stu1280*) of *S. thermophilus* LMG18311 instead of the P23 promoter	This work
pSW4-GFPopt	7.3 kb, Gram-positive/Gram-negative shuttle vector with GFPopt gene; Km^r Ap^r	42
pOri23-pLDH-gfp	pOri23 vector carrying the GFP gene of pSW4-GFPopt under the control of the pLDH promoter of *S. thermophilus* LMG18311	This work

[a]Abbreviations: Cm^r, chloramphenicol resistance; Ery^r, erythromycin resistance; Spc^r, spectinomycin resistance; Km^r, kanamycin resistance; Ap^r, ampicillin resistance.

mutants showed 40- and 100-fold increases of ICE*St3* acquisition ($P < 0.01$, *t* test), respectively, compared to that of a WT recipient strain (Fig. 4A).

(iii) Mating experiments using recipient cells that could be affected in cell surface charge (Δ*mprF*-like and Δ*dltA* mutants). An increase of ICE*St3* acquisition,

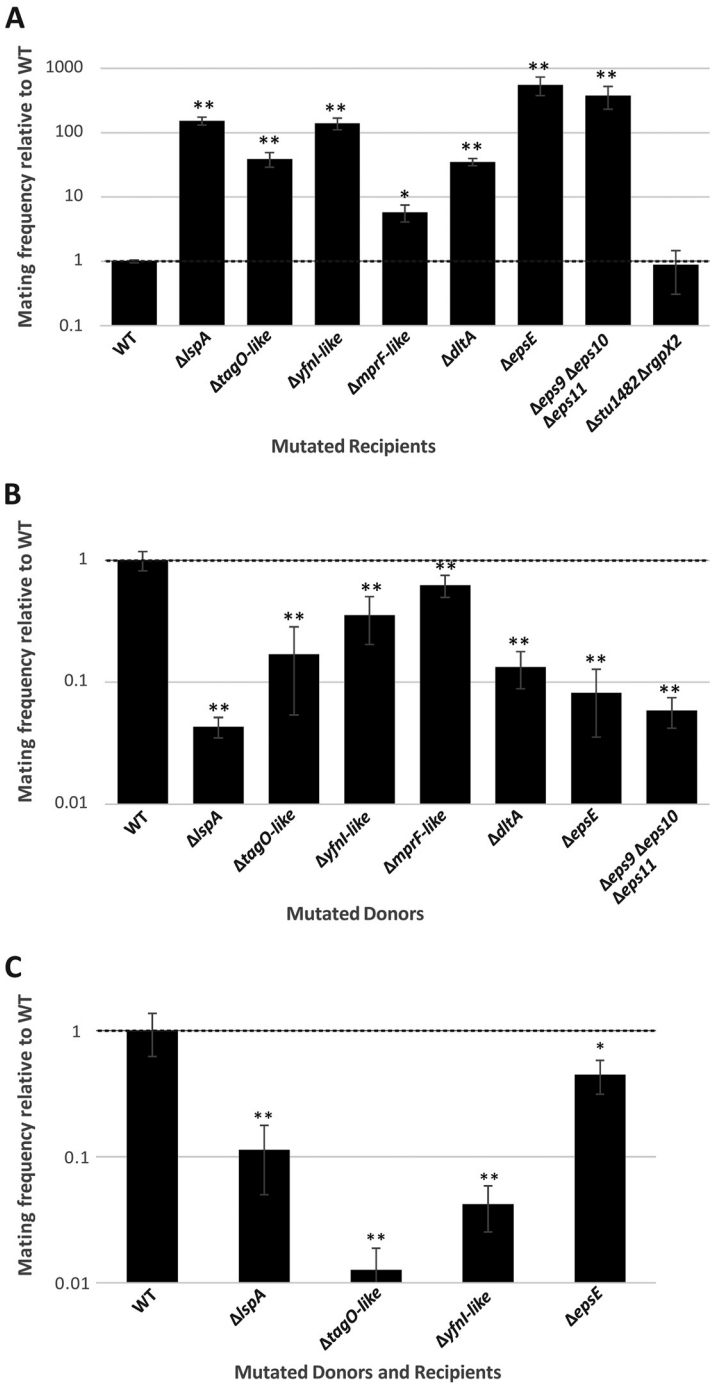

FIG 4 Conjugative transfer of ICE*St3* from and/or to mutants. Conjugation frequencies of LMG 18311 mutants relative to the WT are shown. (A) Conjugative transfer of ICE*St3* using a WT donor and a mutated recipient; (B) conjugative transfer of ICE*St3* using a mutated donor and a WT recipient; (C) conjugative transfer of ICE*St3* using a mutated donor and a mutated recipient. For each experiment, means and standard deviations from at least 3 biological repetitions on 2 independent clones of mutants are shown. * and **, the conjugation frequency is statistically different from that of the WT ($P < 0.05$ and $P < 0.01$, respectively [*t* test]).

albeit lower than those observed for the other mutants (approximately 5-fold [$P < 0.05$, *t* test]), was observed using the Δ*mprF*-like mutant compared to the WT (Fig. 4A). For the Δ*dltA* mutant, an increase similar to the one observed for the WTA mutant (approximately 40-fold [$P < 0.01$, *t* test]) was observed (Fig. 4A).

(iv) Mating experiments using recipient cells affected in cell surface polysaccharide production. A 400-fold increase of ICE*St3* acquisition was obtained for mutants lacking genes or a group of genes belonging to the same cluster and involved in glycosyltransferase activity (*epsE*, *eps11*, and *eps10*), or pyruvyltranferase activity (*eps9*) ($P < 0.01$, *t* test) (Fig. 4A). Under these conditions, the frequency of ICE*St3* transfer was close to 10^{-1} transconjugants per donor. In contrast, a mutant affected in rhamnose-glucose polysaccharide production (Δ*stu1482* Δ*rgpX2*), showed no significant difference in ICE*St3* acquisition compared to WT recipient cells (Fig. 4A).

Conjugative transfer of ICE*St3* using mutated donor cells. In order to investigate whether the phenotypes observed for the mutants are specific to the recipient cells and/or to ICE*St3* activity, mating experiments were also carried out using mutated donor cells. Mating experiments were carried out using selected LMG 18311 mutants (Δ*lspA*, Δ*tagO*-like, Δ*yfnI*-like, Δ*mprF*-like, Δ*dltA*, Δ*epsE*, and Δ*eps9* Δ*eps10* Δ*eps11*) carrying ICE*St3* as donor cells (obtained in the experiments mentioned in the preceding paragraph) and the WT LMG 18311 Spc^r strain as recipient cells (see Table 1). While the mutation of these cell surface molecules in the recipient led to a 5- to 400-fold increase of ICE*St3* acquisition compared to that for the WT, the same mutations in the donor cells led to a significant decrease of ICE*St3* transfer (ranging from less than 10- to 25-fold) compared to that for the WT ($P < 0.01$, *t* test) (Fig. 4B).

Conjugative transfer of ICE*St3* using a mutant/mutant mating pair. To test whether the observed effects of mutations in the donor or recipient cells were additive, mating experiments using mutated donor and recipient cells were also carried out for the Δ*lspA*, Δ*tagO*-like, Δ*yfnI*-like, and Δ*epsE* mutants. The results showed a decrease of ICE*St3* transfer when lipoproteins, teichoic acids, lipoteichoic acids, or exopolysaccharides were affected in both the donor and recipient cells. These results were close to the ones obtained when only the donor strain was mutated. Hence, no additive effect between the donor mutation and the recipient mutation was observed (Fig. 4C).

DISCUSSION

Our results highlight a significant impact of cell surface composition on the conjugation of ICE*St3* of *S. thermophilus*. Indeed, deletion of the *lspA*, *tagO*-like, *yfnI*-like, *dltA*, *epsE*, and *eps9* to *-11* genes in recipient *S. thermophilus* LMG 18311 cells led to an increase of ICE*St3* acquisition. Except for the *eps9* to *-11* cluster, which was found to be specific to *S. thermophilus* LMG 18311, these genes appeared to be highly conserved in *S. thermophilus* and the closely related species *S. salivarius* but also in the more distantly related species *S. pyogenes* and *E. faecalis* (except for *epsE*). It is thus possible that the observed impact on conjugation of these surface molecules could apply to other bacterial species. This indicates that the presence of mature lipoproteins, teichoic acids, and exopolysaccharides at the cell surface can be a hindrance to ICE*St3* acquisition by recipient cells. Taken as a whole, this suggests that the fewer surface molecules, the better conjugation efficiency is, at least when considering the recipient cell. Bearing in mind the important proportion and networks of teichoic acids and exopolysaccharides in the Gram-positive cell surface envelope (20), the lack or decrease of these components could significantly reduce the steric hindrance in the cell envelope. This less congested surface may be suitable for the peptidoglycan hydrolysis activity of the ICE*St3* hydrolase OrfA or for the establishment or activity of the conjugation machinery required for DNA transport in the recipient cell. Furthermore, we cannot exclude that the observed effect of deletions can be linked to the modification of physical-chemical properties of the cell envelope impacting cell-cell interactions and/or DNA transport across the membranes.

Characterization of the mutants revealed some phenotypes that could contribute to the observed impact of mutations on ICE*St3* conjugation. The Δ*lspA* mutant, but also the Δ*tagO*-like, Δ*yfnI*-like, Δ*dltA*, Δ*epsE*, and Δ*eps9* Δ*eps10* Δ*eps11* mutants, showed in particular higher biovolumes and ability of interactions in biofilm assays than the WT. Furthermore, the LMG 18311 Δ*lspA* mutant stood out from the WT and derivatives by

the robustness of its biofilm-forming ability, thus suggesting better cell-to-cell interactions for this mutant.

Lpp. LMG 18311 Δ*lspA* is expected to be affected in its lipoprotein (Lpp) content, as observed in a *Streptococcus sanguinis* Δ*lspA* mutant, whose Lpp show partial activity (35). In *Streptococcus uberis*, the type I signal peptidase Eep seems to replace the cleavage activity of LspA (36), suggesting that an alternative pathway takes place in a Δ*lspA* mutant. Genome analysis of LMG 18311 predicts the presence of two type I signal peptidases (16), but it is not known whether these proteins could be involved in Lpp maturation in a Δ*lspA* mutant context. LMG 18311 Δ*lspA* showed a large increase (up to 100-fold) of ICE*St3* acquisition. LMG 18311 harbors 24 predicted lipoproteins whose presence could interfere with the conjugation machinery assembly. Among these 24 predicted lipoproteins, 15 are involved in the binding of substrates of ABC transporters, whereas others are involved in unknown functions (16). We cannot exclude that a molecular interaction between one or several of these lipoproteins and components of the conjugation machinery could impair ICE*St3* transfer.

WTA. TagO and TarO homologs are described as essential for wall teichoic acid (WTA) biosynthesis in *B. subtilis* (33) and *S. aureus* (37). The LMG 18311 Δ*tagO*-like mutant is thus expected to lack WTA. The Δ*tagO*-like mutant showed an approximately 40-fold increase of ICE*St3* acquisition by recipient cells. TEM analysis revealed that the *tagO* mutant is affected in its septation (this is also true for the *yfnI* mutant). However, it is unclear whether and how this phenotype could contribute to better ICE*St3* acquisition. Contrast and confocal microscopies also indicated that it forms aggregates, as described in other species such as *S. aureus* (37). This phenotype can contribute to better cell-cell interactions.

LTA. The *yfnI*-like gene product is the only lipoteichoic acid (LTA) synthase identified in our *in silico* analysis. Therefore, the disruption of this gene is expected to abrogate, or at least to reduce, LTA presence in the LMG 18311 cell envelope. As in *B. subtilis* for ICE*Bs1* acquisition (9), the Δ*yfnI*-like mutant of *S. thermophilus* LMG 18311 showed an increased propensity for ICE*St3* acquisition. The much higher impact of the *yfnI*-like mutation on ICE*St3* transfer (approximately 100-fold) than on ICE*Bs1* acquisition (less than 10-fold) could be explained by the fact that two additional enzymes, $LtaS_{BS}$ and YqgS, are involved with YfnI in LTA biosynthesis in *B. subtilis* (24). Thus, *yfnI* deletion in these species is not expected to trigger the same phenotypes. This can also be linked to the difference of transfer frequency between ICE*Bs1* and ICE*St3*, thus making ICE*Bs1* more prone to saturation.

We also investigated the impact of an *mprF* mutation on ICE*St3* acquisition by the recipient cells. Unlike the case for ICE*Bs1* and Tn*916* (8), the Δ*mprF*-like mutant showed an increase of ICE*St3* acquisition, although to a lesser extent than for the other mutants. As suggested by Johnson and Grossman, MprF, which impacts the level of lysyl-phosphatidylglycerol, a positively charged molecule, could be involved in cell buffering under the various environmental conditions encountered by the bacteria (9). Specific environmental growth conditions and cell surface charge of *S. thermophilus* could explain these observed differences, suggesting a species-dependent impact of lysyl-phosphatidylglycerol on conjugation.

D-Alanylation of teichoic acid content. WTA and LTA are known to be negatively charged polymers; however, little is known about the cell envelope composition of *S. thermophilus* regarding its teichoic acid content. One hypothesis could be that the observed impacts on ICE*St3* transfer and acquisition are partly linked to the negative charges carried by the WTA and LTA polymers. The absence of these molecules would make the cell envelope less negatively charged, hence contributing to better interactions with the donor that is negatively charged. To test whether WTA and LTA impacts are linked to cell surface charge, ICE*St3* transfers were assessed using a Δ*dltA* mutant as the recipient. The *dltA* gene belongs to the *dlt* operon, which is responsible for the D-alanylation of both WTA and LTA, thus neutralizing their negative charge and making the whole polymers zwitterionic, or at least reducing them. It has been described that

a *dltA* mutation is sufficient to impair D-alanylation of WTA and LTA in *B. subtilis* (26). Thus, LMG 18311 Δ*dltA* is expected to have fully negatively charged WTA and LTA polymers exposed at its surface. However, the Δ*dltA* mutant showed an increase of ICE*St3* acquisition similar to that for a Δ*tagO*-like mutant (approximately a 40-fold increase for both compared to the WT) but lower than that for the Δ*yfnI*-like mutant (approximately a 100-fold increase compared to the WT), which is not consistent with this hypothesis. However, we cannot exclude that the Δ*dltA* effect could be due to the lack of D-alanylation of another cell envelope component. Furthermore, no measurable difference of zeta potential was detected between the WT, Δ*dltA*, Δ*tagO*-like, and Δ*yfnI*-like strains under the tested conditions, suggesting that the change of surface charge is minor in these mutants, which can be explained by the following hypotheses: (i) LTA and WTA in *S. thermophilus* LMG 18311 could harbor a carbon backbone poorly loaded in phosphoglycerol repeat units, and (ii) LMG 18311 could display small amounts of LTA and WTA at its surface, thus explaining the absence of a significant change in the cell surface net charge. However, this could also indicate that not all teichoic acids were removed by these mutations. These results also highlight that the increase of ICE*St3* acquisition observed when recipient is affected in WTA or LTA biosynthesis is not linked to the negative charges that both these polymers could confer to the bacteria. Moreover, the same impact on ICE*St3* acquisition observed for both the Δ*dltA* and Δ*tagO*-like mutants could be linked to the formation of aggregates that could improve cell-to-cell interactions of both mutants. Indeed, these mutants form mixed aggregates with donor cells carrying a green fluorescent protein (GFP) gene-labeled ICE when examined by confocal microscopy (see Fig. S3 in the supplemental material for the Δ*tagO*-like mutant).

EPS. Several genes belonging to a large gene cluster involved in exopolysaccharide (EPS) biosynthesis were mutated in LMG 18311. These mutants showed the greatest increase of ICE*St3* acquisition, with a transfer frequency reaching 10^{-1} transconjugants per donor. Unlike *S. thermophilus* teichoic acids, EPS are well documented, and it has been described that the lack of the EpsE glycosyltransferase leads to a lack of EPS at the *S. thermophilus* cell surface (32). We confirmed this observation by SEM and TEM, since EPS is absent from the cell surfaces of Δ*epsE* and Δ*eps9* Δ*eps10* Δ*eps11* mutants. Liquid culture of these mutants showed sedimentation following growth, which could be a consequence of the cell chain length increase of these mutants compared to the WT. This increase in chain length likely facilitates ICE retransfer within the same chain of recipient cells, as described for *B. subtilis* (38), and could thus artificially increase the frequency of ICE*St3* transfer. However, we found, by counting CFU before and after vortexing, that the vortexing step used in the conjugation experiments is not sufficient to disrupt cell chains of *S. thermophilus* LMG 18311. This indicates that, in our experiments, retransfer events are not counted in the conjugation frequency and do not explain the observed increase of ICE*St3* transfer. EPS mutants show a significant change in cell surface charge compared to the WT and the other mutants. This phenotype could originate from the presence of phosphate and acetate components that may be attached to the EPS backbone. It could be hypothesized that these changes in electrostatic cell interactions favor ICE*St3* acquisition.

LPXTG proteins. the mutation of *srtA* in LMD-9 did not have any significant impact regarding ICE*St3* acquisition compared to that of the WT, thus suggesting that the covalent linkage of LPXTG proteins to the cell membrane does not interfere with DNA transport inside the recipient cell.

Mutations affecting cell surface composition were also tested in a donor context (except for the Δ*stu1482* Δ*rgpX2* mutant) instead of a recipient one. Δ*lspA*, Δ*tagO*-like, Δ*yfnI*-like, Δ*epsE*, and Δ*eps9* Δ*eps10* Δ*eps11* donor mutants were not able to efficiently transfer ICE*St3* toward WT recipient cells. Our results indicate that the impact of mutations is different when the donor cell is targeted. Since the same strain was used, this difference in behavior is likely linked to the donor or recipient "status" in link with ICE*St3* activity. The transfer frequencies of ICE*St3* using Δ*lspA*, Δ*tagO*-like, Δ*yfnI*-like, and

Δ*epsE* mutant donors also decreased when using recipient cells carrying the same mutation (mutant/mutant pairs).

No obvious additive effect between donor and recipient mutations was observed, thus suggesting that (i) the effect of a donor mutation is dominant and (ii) the adverse effect occurs prior to ICE*St3* entry in the recipient cell. These results suggest that lipoproteins, wall teichoic acids, lipoteichoic acids, and exopolysaccharides are important for the proper positioning/assembly or activity of the conjugation machinery in the donor cell.

This study contributes to a better understanding of the impact of host factors on conjugation, but further studies are needed to decipher precisely how these factors interfere with the transfer of conjugative elements.

MATERIALS AND METHODS

Bacterial strains and culture conditions. The strains used in this study are listed in Table 1. *S. thermophilus* LMG 18311, LMD-9, and their derivatives were grown in M17 broth supplemented with 0.5% lactose (LM17) at 42°C without shaking. When required, cultures were supplemented with antibiotics at the following concentrations: chloramphenicol, 6 μg ml^{-1}; erythromycin, 5 μg ml^{-1}; and spectinomycin, 500 μg ml^{-1}.

Genome analysis. A search for homologs of *B. subtilis* proteins involved in WTA (33), LTA (24), and lysyl-phosphatidylglycerol (19) biosynthesis was carried out on the *S. thermophilus* LMG 18311 genome using the blastp program (with default parameters and low-complexity filter disabled). This genome was also screened for the presence of annotated clusters encoding polysaccharides and exopolysaccharides. Eight genes or clusters of genes were selected for mutant construction: *stu0163* (homolog of *tagO* of *B. subtilis*), *stu0521* (*lspA* gene), *stu0636* (homolog of *yfnI* of *B. subtilis*), *stu0761* (*dltA* gene), *stu1256* (homolog of *mprF* of *B. subtilis*), *stu1108* (encoding EpsE, the major glycosyltransferase involved in exopolysaccharide synthesis in *S. thermophilus*), 1 cluster encoding exopolysaccharides (*stu1097*, *stu1097*, and *stu1099*), and a cluster encoding rhamnose (*stu1473*, *stu1480*, *stu1481*, and *stu1482*).

All the genomes available in GenBank (last interrogation, 3 November 2017) for *S. thermophilus* (19 complete and 18 draft genomes), the closely related *S. salivarius* species (9 complete and 33 draft genomes), and the two species that successfully acquired ICE*St3*, *S. pyogenes* (60 complete and 297 draft genomes) and *E. faecalis* (15 complete and 533 draft genomes), were searched for homologs of these genes or clusters of genes with the tBLASTn program (with default parameters and low-complexity filter disabled). Hits were retained when they showed more than 50% of query cover and more than 40% of amino acid identity with the query proteins of *S. thermophilus* LMG 18311.

Construction of mutants affected in cell surface composition. *S. thermophilus* LMG 18311 (WT) was used to construct cell surface mutants. For each targeted molecule, the gene sequence was deleted by insertion of an erythromycin resistance cassette by overlap PCR as described previously (39). PCRs were performed with 50 ng of genomic DNA, 200 μM each deoxynucleoside triphosphate (dNTP), 0.5 μM each primer (primer sequences are given in Table 2), and 0.02 U μl^{-1} of Phusion high-fidelity DNA polymerase (Thermo Scientific) in appropriate buffer per 50-μl reaction volume. Cycling conditions for the overlap PCR were 3 min at 98°C, 30 s at the annealing temperature (with a 1°C increment at each cycle), and 30 s/kb at 72°C, followed by 30 additional cycles with an annealing temperature of 55°C and a final extension of 10 min at 72°C. PCR products were then used for natural transformation of LMG 18311. The same steps were followed for chromosomal tagging of strain LMG 18311 with two different resistance genes (erythromycin or spectinomycin resistance gene) (Table 1). These resistance cassettes were inserted in an intergenic region between two convergent open reading frames (ORFs) in the *S. thermophilus* genome (14), *stu0627* and *stu0629*. LMD-9(pMG36e) was obtained by natural transformation of LMD-9 with purified extract of pMG36e using a previously described protocol (39).

The pSL1180 spec vector was obtained by cloning an SpeI-SpeI spectinomycin resistance cassette at the AvrII site of pSL1180. The SpeI-SpeI spectinomycin resistance cassette was amplified from the pSET4S plasmid using the Spec-lox71-SpeI F and Spec-lox66-SpeI R primers (Table 2), which introduce SpeI sites upstream and downstream the resistance cassette.

Mating experiments. *S. thermophilus* LMG 18311 was chosen for mating experiments. This strain was previously successfully used as a recipient for ICE*St3* using the original donor strain CNRZ385 (at a frequency of 10^{-6} transconjugants per donor), but it can also act as a donor transferring ICE*St3* at the same frequency (11). In order to avoid interference with host factors, LMG 18311 was used as both donor and recipient in mating experiments. Depending on the mating pair used, derivatives of strain LMG 18311, tagged with either an erythromycin or a spectinomycin resistance gene, were used as recipients (Table 1). The mating pair using the LMG 18311(ICE*St3*) donor strain with these recipient strains was considered a WT mating pair (with an ICE*St3* transfer frequency of 10^{-4} transconjugants per donor), and the term mutant was used for the cells affected in their cell surface composition.

Donor and recipient strains were grown overnight with an appropriate antibiotic. Fifteen milliliters of broth medium was inoculated with 150 μl of donor or recipient stationary-phase cultures. Cultures were grown until mid-exponential phase (optical density at 600 nm [OD_{600}] of 0.4) and then were mixed and centrifuged for 15 min in a prewarmed centrifuge at 4,200 $\times$ *g* to pellet cells. The pellet was resuspended in 1 ml of LM17 broth, and 150 μl was spread on 0.45-μm-pore-size cellulose nitrate filters (Millipore) deposited on LM17 soft agar (0.8%) plates. The plates were then incubated at 42°C. After an overnight

TABLE 2 Primers used in this work

Primer use	Primer name	Sequence (5′→3′)
LMG 18311 Ery^r construction	MchromLMG I_Fwd	GAGGAACTCGGATTGGTAG
	MchromLMG I_rev_ery	AGCCATCCGGAAGATCTGGGACCATTTCGTTTGCAC
	MchromLMG II_fwd_ery	AACACGAACCGTCTTATCTCCCAACTTAATTGAAGGCCAT
	MchromLMG II_Rev	CAGGGCTAGCTATTGTTTC
	Prom-Ery-For	GGAGATAAGACGGTTCGTGTT
	pSL1180 ery rev	CAGATCTTCCGGATGGCT
LMG 18311 Spc^r construction	MchromLMG I_Fwd	GAGGAACTCGGATTGGTAG
	MchromLMG I_rev_spc	GGGAAATATTCATTCTAATTGGGGACCATTTCGTTTGCAC
	MchromLMG II_fwd_spc	ATTTATAGATTTCATTGGCTTCCAACTTAATTGAAGGCCAT
	MchromLMG II_Rev	CAGGGCTAGCTATTGTTTC
	SpecFwd	TAGAAGCCAATGAAATCTAT
	Speclox66 Rev	CCAATTAGAATGAATATTTCCC
LMG 18311 Δ*lspA* construction	EG1885	ACGAGTACTTCTTGACAGACAAATCAGA
	EG1886	TCATGTAATCACTCCTTCTTAATTACACATAAGTCCTCCTATGGTTTATAAGTATCA
	EG1887	TATTTAACGGGAGGAAATAATTCTACATTAAAGAGGCGGGAAACCGTCTGGACAAGT
	EG1888	AGAACATCCGTTGGATGACTATTAAGCT
LMG 18311 Δ*tagO*-like construction	EG1873	ATAGGCAGTCATGGTTGTTACCTCC
	EG1874	TCATGTAATCACTCCTTCTTAATTACACATGTCCTAGCTCCATTTCGTTGCTTGT
	EG1875	TATTTAACGGGAGGAAATAATTCTAAAATAAACATTTGAAAAGCCAAGCAATGGCT
	EG1876	AGATCTTGCAACCAGAGTGGCTCTGCT
LMG 18311 Δ*yfnI*-like construction	EG1897	TCCATACTAAAGCCATTAGCTTCAAA
	EG1898	TCATGTAATCACTCCTTCTTAATTACACAAAATAATACTTCCTTTGATTTCATATTA
	EG1899	TATTTAACGGGAGGAAATAATTCTAGAATAATCCTAAAAAGACTGTTCTAAT
	EG1900	ACTTGACTGTGCATCATCTGAATTCTA
LMG 18311 Δ*mprF*-like construction	EG1951	TCATTTATGGTATCTAAGCTTGTCCGT
	EG1902	TCATGTAATCACTCCTTCTTAATTACACATGCCACCACCTCTTTTTGACTAATTCTA
	EG1903	TATTTAACGGGAGGAAATAATTCTAAAGTAAATACGACAAAAAAAGTGACCCTCCAGGGTT
	EG1904	AGCATTCTCGATATGGATATTCCTGA
LMG 18311 Δ*dltA* construction	EG1947	AGTGCTTTAGCCTGTGCTGATCGTCTA
	EG1914	TCATGTAATCACTCCTTCTTAATTACACATTATTCTTCCTAAAATTCGTTATAGATA
	EG1915	TATTTAACGGGAGGAAATAATTCTACGATGATAGACTTCTTGAAACAGCTTCCCC
	EG1916	TCGCATGAGTACTATGACTAAGCGCATA
LMG 18311 Δ*epsE* construction	EG1945	ACTAAGGTTGATAAGAACAATATCGAGA
	EG1946	TCATGTAATCACTCCTTCTTAATTACACACTTATTTTTCCTCCATCAGATTTTTGAT
	EG1923	TATTTAACGGGAGGAAATAATTCTAAAATGATAACTTCAAAGATGATTAGATGAG
	EG1924	AGACCTGTAATTCCTGGCTTGAAGCT
LMG 18311 Δ*eps9* Δ*eps10* Δ*eps11* construction	EG1941	AGGAATGTCAAGATTTAGGAATTACA
	EG1942	TCATGTAATCACTCCTTCTTAATTACACATCTTCTCATCACCTAAATATTGATTTTT
	EG1943	TATTTAACGGGAGGAAATAATTCTACAATAAATTCAATGATAATATAAGAGTTGC
	EG1944	TTGCTAAATGCTGAGTAAATCCATTCCA
LMG 18311 Δ*stu1482* Δ*rgpX2* construction	EG1937	TGGTATTGATAGTATCGAAAGTAGAGA
	EG1938	TCATGTAATCACTCCTTCTTAATTACACATTTTTATACGTAGTTTCTCCTGAAAACT
	EG1939	TATTTAACGGGAGGAAATAATTCTAAAATAATATTTTATTAATAGCAGTCCCCTG
	EG1940	ATCAGTTTGTGCCATAGCCTCCAGTA
Ery resistance cassette used for mutant construction	EG940	TGTAATTAAGAAGGAGTGA
	EG941	TAGAATTATTTCCTCCCGT
pSL1180 spec lox vector construction	Spec-lox71-SpeI F	TTTTTACTAGTTCGTACCGTTCGTATAGCATACATTATACGAAGTTATCGTAACGTG ACTGGCAAGA
	Spec-lox66-SpeI R	TTTTTACTAGTCGTACCGTTCGTATAATGTATGCTATACGAAGTTATCCAATTAGAA TGAATATTTCCC
pOri23-pLDH-gfp vector construction	PLDHthermo-fwd-EcoRI	TTTTTGAATTCTTTCAATCAAATTATTCC
	PLDHthermo-rev-BamHI-SacI	TTTTTGGATCCGTTGCAGTCATGAGCTCAACATCTC
	gfp-fwd-SacI	TTTTTGAGCTCATGTCATGTCAAAAGAATTA
	gfp-rev-PstI	GATAAGCTTGGCTGCAGGT
	pldh_oe_fwd	GGAGATTGAGCATACCTAGGGGAATTCTTTCAATCAAATTATTCC
	gfp-oe-rev	CGGTGACTAGTTATCTACACGGATAAGCTTGGCTGCAGG

incubation, the filters were removed from the agar plates and placed into 10 ml of LM17 liquid medium. Bacteria were recovered by vortexing for 30 s. By counting CFU before and after vortexing, we showed that such a short vortexing step is not sufficient to disrupt cell chains of *S. thermophilus* LMG 18311 (data not shown). The suspension was then directly spread on agar plates supplemented with the appropriate antibiotic to enable counting the CFU of the donor, recipient, and transconjugant cells after a 24-h incubation.

Mating frequencies were calculated by dividing the number of transconjugants by the number of donor CFU. At least three independent biological repetitions were done on two independent transformants. Statistical analysis was carried out by using Student's *t* test.

Sedimentation tests. Sedimentation of the LMG 18311 Δ*epsE* and Δ*eps9* Δ*eps10* Δ*eps11* mutants was visualized after 8 h of growth in LM17 liquid culture and was compared to that of WT LMG 18311. The cultures were observed by phase-contrast microscopy with an original magnification of ×400.

Determination of bacterial cell wall zeta potential. Bacterial cells from overnight cultures were harvested by centrifugation (5 min at 7,000 × *g*), washed twice with demineralized water, and suspended in demineralized water. To break bacterial chains, cells were vortexed for 3 min. Electrophoretic mobility measurements were done by suspending the bacterial strains in 3 ml of 10 mM potassium phosphate buffer with the pH ranging from 2 to 9 to obtain an OD_{600} of 0.07. The electrophoretic mobility at 150 V of the suspended bacteria was then measured using the ZetaSizer Nano ZS apparatus (Malvern Instruments Ltd., Malvern, UK). Electrophoretic mobilities were converted to the zeta potentials using the Helmholtz-Smoluchowski equation. At least three independent biological replicates were done.

TEM. For each strain, 50 ml of planktonic bacteria grown until the end of exponential growth was pelleted at 2,000 rpm for 10 min at 4°C. Samples were then fixed for 1 h at room temperature in a 0.1 M cacodylate buffer containing 2% (vol/vol) glutaraldehyde (pH 7.2). Samples were kept overnight at 4°C in a 0.1 M cacodylate and 0.2 M sucrose buffer. Bacteria were then washed one time during 5 min with 0.1 M cacodylate buffer, contrasted during 1 h with 0.5% Oolong tea extract (OTE) in 0.1 M cacodylate buffer, and washed 2 times during 5 min with 0.1 M cacodylate buffer. Samples were postfixed for 1 h at room temperature in 0.1 M cacodylate buffer containing 1% (vol/vol) osmium tetroxide with 1.5% potassium cyanoferrate and then washed twice for 5 min with distilled water. Thereafter, cells were dehydrated in a gradual ethanol series (30%, 50%, 70%, and 90% [vol/vol] with distilled water and 3 times with 100% ethanol, 10 min for each step, except overnight for 70% ethanol). A 10-min intermediate bath in propylene oxide was performed. The bacteria were then impregnated at room temperature in successive mixes of propylene oxide and Epon (2:1; 1:1, and 1:2; each step for 2 h), in pure Epon overnight, and under vacuum conditions. A final inclusion bath with pure Epon and dimethylaminoethanol (DMAE) (an accelerator) was performed, and polymerization was allowed by incubating for 48 h at 60°C. Ultrathin sections of 70 nm were cut with an ultramicrotome (UC6; Leica, Germany) and deposited on 200-mesh copper-platinum grids. Sections were stained for 2 min in Reynold's lead citrate and rinsed in distilled water. Observations were performed using an HT7700 transmission electron microscope (Hitachi, Japan) equipped with an 8-million-pixel format charge-coupled device (CCD) camera driven by the image capture engine software AMT, version 6.02, at the INRA MIMA2 microscopy platform (Jouy-en-Josas, France). Images were made at 80 kV in high-contrast mode with an objective aperture adjusted for each sample and magnification.

SEM. Bacterial suspensions, collected at the end of exponential growth, were immersed in a fixative solution (2.5% glutaraldehyde in 0.2 M sodium cacodylate buffer, pH 7.4), deposited on sterile cover glass discs (Marienfeld, VWR, France), and stored for 1 h at room temperature and overnight at 4°C. The fixative was removed, and samples were rinsed three times for 10 min each in the sodium cacodylate solution (pH 7.4). The samples underwent progressive dehydration by soaking in a gradual ethanol series (50 to 100%) before critical-point drying under CO_2. Samples were mounted on aluminum stubs (10-mm diameter) with carbon adhesive discs (Agar Scientific; Oxford Instruments SAS, Gometz-La-Ville, France) and sputter coated with platinum (Polaron SC7640; Elexience, Verrières-le-Buisson, France) for 200 s at 10 mA. Samples were visualized by field emission gun scanning electron microscopy (SEM). They were viewed as secondary electron images (2 kV) with a Hitachi S4500 instrument (Elexience, Verrières-le-Buisson, France). Scanning electron microscopy analyses were performed at the Microscopy and Imaging Platform MIMA2 (INRA, Jouy-en-Josas, France).

Biofilms assays by laser scanning confocal microscopy. Biofilms were measured in polystyrene 96-well microtiter plates with a μclear base (Greiner Bio-One, France), enabling high-resolution fluorescence imaging, as previously described (40). A volume of 200 μl of an overnight culture in LM17 (adjusted to an optical density at 600 nm of 0.01) was added to the wells of a microtiter plate. The microtiter plate was then kept at 42°C for 60 min to allow the bacteria to adhere to the bottom of the wells. After this adhesion step, the wells were rinsed with the growth medium to eliminate any nonadherent bacteria and then refilled with 200 μl of LM17. The microtiter plate was then incubated at 42°C for 2, 6, or 15 h and rinsed or not with a microplate autowasher (Thermo Fisher Wellwash) before microscopic evaluation. Bacterial cells were fluorescently stained in green with the nucleic acid marker SYTO9 (1:500 dilution in LM17 from a SYTO9 stock solution at 5 mM in dimethyl sulfoxide [DMSO]; Invitrogen, France). After 20 min of incubation in the dark to enable fluorescent labeling of the bacteria, the plate was mounted on the motorized stage of the confocal microscope (Leica SP8 AOBS inverter confocal laser scanning microscope at the MIMA2 platform, http://www6.jouy.inra.fr/mima2_eng/). The microtiter plates were scanned using a 63×/1.2-numerical-aperture (NA) water immersion objective lens and scanned at excitation wavelengths of 488 nm (argon laser; 3% intensity), with emission wavelengths collected from 493 to 550 nm using hybrid detectors (HyD Leica Microsystems, Germany). Three-dimensional (3D) projections of the biofilm structures before and after the washing

step were reconstructed using the Easy 3D function of the IMARIS software (Bitplane, Switzerland). The biofilm biovolume is defined as the number of biomass pixels in all images of a stack multiplied by the voxel size and divided by the substratum area of the image stack (41). The biofilm biovolume (in μm^3) was automatically extracted from image series using the dedicated ImageJ COMSTAT2 plugin (www.comstat.dk) (41).

Analysis of aggregates by laser scanning confocal microscopy. Cells of *S. thermophilus* LMG 18311 carrying ICE*St3* were discriminated by labeling ICE*St3* with a GFP gene. A pOri23-pLDH vector was first constructed by cloning the promoter of the L-lactate dehydrogenase gene from *S. thermophilus* LMG 18311 (*stu1280*) in the pOri23 plasmid using the PLDHthermo-fwd-EcoRI and PLDHthermo-rev-BamHI-SacI primers (Table 2). The GFP gene, encoding a green fluorescent protein that was codon optimized for low-GC Gram-positive bacteria, was amplified by PCR with the gfp-fwd-SacI and gfp-rev-PstI primers using the pSW4-GFPopt plasmid constructed by Sastalla et al. (42) and then cloned downstream of the pLDH promoter in the pOri23-pLDH vector after digestion by the SacI and PstI restriction enzymes to give pOri23-pLDH-gfp (Table 1). The pLDH-gfp fragment was then amplified by PCR using primers that introduce extensions matching sequences of ICE*St3* (pldh_oe_fwd and gfp-oe-rev). This enables synthesis of an overlap PCR fragment carrying the pLDH-gfp cassette flanked by sequences of ICE*St3*. After induction of natural competence of *S. thermophilus* cells, the overlap PCR product was then added for transformation. The crossover events, upstream and downstream from the tagged region, were positively selected by the newly acquired fluorescence of the transformed clones.

Cells carrying ICE*St3-gfp* (LMG 18311 ICE*St3* pLDH-gfp) were mixed with LMG 18311 WT or mutants (Δ*tagO*-like or Δ*dltA*) and incubated for 4 to 6 h at 42°C before observation. Cells were counterlabeled using the syto61 red fluorescent nucleic acid stain before observation by confocal microscopy using a Leica SP8 AOBS inverter confocal laser scanning microscope at the MIMA2 platform (http://www6.jouy.inra.fr/mima2_eng/).

SUPPLEMENTAL MATERIAL

Supplemental material for this article may be found at https://doi.org/10.1128/AEM.02109-17.

SUPPLEMENTAL FILE 1, PDF file, 0.3 MB.

ACKNOWLEDGMENTS

We thank Sophie Bobet and Johan Staub for the construction of mutant strains, Alexis Canette for TEM observations, Steve Leppla of the Laboratory of Bacterial Diseases of the National Institute of Allergy and Infectious Diseases (Bethesda, MD, USA) for providing the pSW4-GFPopt vector, and UR AFPA laboratory for providing the *srtA* mutant.

N.D. is the recipient of a scholarship funded by INRA and Région Grand Est. This work received financial support from the Région Lorraine and Université de Lorraine (2011 to 2013) and from ANR (MATICE project, ANR-15-CE21-0007).

REFERENCES

1. Koonin EV. 2016. Horizontal gene transfer: essentiality and evolvability in prokaryotes, and roles in evolutionary transitions. F1000Res 5:F1000 Faculty Rev-1805. https://doi.org/10.12688/f1000research.8737.1.
2. Garcia-Aljaro C, Balleste E, Muniesa M. 2017. Beyond the canonical strategies of horizontal gene transfer in prokaryotes. Curr Opin Microbiol 38:95–105. https://doi.org/10.1016/j.mib.2017.04.011.
3. Llosa M, Gomis-Ruth FX, Coll M, de la Cruz Fd F. 2002. Bacterial conjugation: a two-step mechanism for DNA transport. Mol Microbiol 45:1–8. https://doi.org/10.1046/j.1365-2958.2002.03014.x.
4. Bellanger X, Payot S, Leblond-Bourget N, Guedon G. 2014. Conjugative and mobilizable genomic islands in bacteria: evolution and diversity. FEMS Microbiol Rev 38:720–760. https://doi.org/10.1111/1574-6976.12058.
5. Delavat F, Miyazaki R, Carraro N, Pradervand N, van der Meer JR. 2017. The hidden life of integrative and conjugative elements. FEMS Microbiol Rev 41:512–537. https://doi.org/10.1093/femsre/fux008.
6. Johnson CM, Grossman AD. 2015. Integrative and conjugative elements (ICEs): what they do and how they work. Annu Rev Genet 49:577–601. https://doi.org/10.1146/annurev-genet-112414-055018.
7. Carraro N, Burrus V. 2014. Biology of three ICE families: SXT/R391, ICE*Bs1*, and ICE*St1*/ICE*St3*. Microbiol Spectr 2:1–20. https://doi.org/10.1128/microbiolspec.MDNA3-0008-2014.
8. Johnson CM, Grossman AD. 2014. Identification of host genes that affect acquisition of an integrative and conjugative element in *Bacillus subtilis*. Mol Microbiol 93:1284–1301. https://doi.org/10.1111/mmi.12704.
9. Johnson CM, Grossman AD. 2016. The composition of the cell envelope affects conjugation in *Bacillus subtilis*. J Bacteriol 198:1241–1249. https://doi.org/10.1128/JB.01044-15.
10. Hong TP, Carter MQ, Struffi P, Casonato S, Hao Y, Lam JS, Lory S, Jousson O. 2017. Conjugative type IVb pilus recognizes lipopolysaccharide of recipient cells to initiate PAPI-1 pathogenicity island transfer in *Pseudomonas aeruginosa*. BMC Microbiol 17:31. https://doi.org/10.1186/s12866-017-0943-4.
11. Bellanger X, Roberts AP, Morel C, Choulet F, Pavlovic G, Mullany P, Decaris B, Guedon G. 2009. Conjugative transfer of the integrative conjugative elements ICE*St1* and ICE*St3* from *Streptococcus thermophilus*. J Bacteriol 191:2764–2775. https://doi.org/10.1128/JB.01412-08.
12. Carraro N, Libante V, Morel C, Decaris B, Charron-Bourgoin F, Leblond P, Guedon G. 2011. Differential regulation of two closely related integrative and conjugative elements from *Streptococcus thermophilus*. BMC Microbiol 11:238. https://doi.org/10.1186/1471-2180-11-238.
13. Delorme C, Abraham AL, Renault P, Guedon E. 2015. Genomics of *Streptococcus salivarius*, a major human commensal. Infect Genet Evol 33:381–392. https://doi.org/10.1016/j.meegid.2014.10.001.
14. Bolotin A, Quinquis B, Renault P, Sorokin A, Ehrlich SD, Kulakauskas S, Lapidus A, Goltsman E, Mazur M, Pusch GD, Fonstein M, Overbeek R, Kyprides N, Purnelle B, Prozzi D, Ngui K, Masuy D, Hancy F, Burteau S, Boutry M, Delcour J, Goffeau A, Hols P. 2004. Complete sequence and comparative genome analysis of the dairy bacterium *Streptococcus thermophilus*. Nat Biotechnol 22:1554–1558. https://doi.org/10.1038/nbt1034.

15. Couvigny B, Therial C, Gautier C, Renault P, Briandet R, Guedon E. 2015. *Streptococcus thermophilus* biofilm formation: a remnant trait of ancestral commensal life? PLoS One 10:e0128099. https://doi.org/10.1371/journal.pone.0128099.
16. Hols P, Hancy F, Fontaine L, Grossiord B, Prozzi D, Leblond-Bourget N, Decaris B, Bolotin A, Delorme C, Dusko Ehrlich S, Guedon E, Monnet V, Renault P, Kleerebezem M. 2005. New insights in the molecular biology and physiology of *Streptococcus thermophilus* revealed by comparative genomics. FEMS Microbiol Rev 29:435–463.
17. Siegel SD, Reardon ME, Ton-That H. 2017. Anchoring of LPXTG-like proteins to the Gram-positive cell wall envelope. Curr Top Microbiol Immunol 404:159–175. https://doi.org/10.1007/82_2016_8.
18. Buddelmeijer N. 2015. The molecular mechanism of bacterial lipoprotein modification—how, when and why? FEMS Microbiol Rev 39:246–261. https://doi.org/10.1093/femsre/fuu006.
19. Parsons JB, Rock CO. 2013. Bacterial lipids: metabolism and membrane homeostasis. Prog Lipid Res 52:249–276. https://doi.org/10.1016/j.plipres.2013.02.002.
20. Burgain J, Scher J, Francius G, Borges F, Corgneau M, Revol-Junelles AM, Cailliez-Grimal C, Gaiani C. 2014. Lactic acid bacteria in dairy food: surface characterization and interactions with food matrix components. Adv Colloid Interface Sci 213:21–35. https://doi.org/10.1016/j.cis.2014.09.005.
21. Chapot-Chartier MP, Kulakauskas S. 2014. Cell wall structure and function in lactic acid bacteria. Microb Cell Fact 13(Suppl 1):S9. https://doi.org/10.1186/1475-2859-13-S1-S9.
22. Schade J, Weidenmaier C. 2016. Cell wall glycopolymers of Firmicutes and their role as nonprotein adhesins. FEBS Lett 590:3758–3771. https://doi.org/10.1002/1873-3468.12288.
23. Grundling A, Schneewind O. 2007. Synthesis of glycerol phosphate lipoteichoic acid in *Staphylococcus aureus*. Proc Natl Acad Sci U S A 104:8478–8483. https://doi.org/10.1073/pnas.0701821104.
24. Wormann ME, Corrigan RM, Simpson PJ, Matthews SJ, Grundling A. 2011. Enzymatic activities and functional interdependencies of *Bacillus subtilis* lipoteichoic acid synthesis enzymes. Mol Microbiol 79:566–583. https://doi.org/10.1111/j.1365-2958.2010.07472.x.
25. Miyauchi E, Morita M, Rossi M, Morita H, Suzuki T, Tanabe S. 2012. Effect of D-alanine in teichoic acid from the *Streptococcus thermophilus* cell wall on the barrier-protection of intestinal epithelial cells. Biosci Biotechnol Biochem 76:283–288. https://doi.org/10.1271/bbb.110646.
26. Perego M, Glaser P, Minutello A, Strauch MA, Leopold K, Fischer W. 1995. Incorporation of D-alanine into lipoteichoic acid and wall teichoic acid in *Bacillus subtilis*. Identification of genes and regulation. J Biol Chem 270:15598–15606.
27. Rehm BH. 2010. Bacterial polymers: biosynthesis, modifications and applications. Nat Rev Microbiol 8:578–592. https://doi.org/10.1038/nrmicro2354.
28. Schmid J, Sieber V, Rehm B. 2015. Bacterial exopolysaccharides: biosynthesis pathways and engineering strategies. Front Microbiol 6:496. https://doi.org/10.3389/fmicb.2015.00496.
29. De Vuyst L, Weckx S, Ravyts F, Herman L, Leroy F. 2011. New insights into the exopolysaccharide production of *Streptococcus thermophilus*. Int Dairy J 21:586–591. https://doi.org/10.1016/j.idairyj.2011.03.016.
30. Pachekrepapol U, Lucey JA, Gong Y, Naran R, Azadi P. 2017. Characterization of the chemical structures and physical properties of exopolysaccharides produced by various *Streptococcus thermophilus* strains. J Dairy Sci 100:3424–3435. https://doi.org/10.3168/jds.2016-12125.
31. Ren W, Xia Y, Wang G, Zhang H, Zhu S, Ai L. 2016. Bioactive exopolysaccharides from a *S. thermophilus* strain: screening, purification and characterization. Int J Biol Macromol 86:402–407. https://doi.org/10.1016/j.ijbiomac.2016.01.085.
32. Minic Z, Marie C, Delorme C, Faurie JM, Mercier G, Ehrlich D, Renault P. 2007. Control of EpsE, the phosphoglycosyltransferase initiating exopolysaccharide synthesis in *Streptococcus thermophilus*, by EpsD tyrosine kinase. J Bacteriol 189:1351–1357. https://doi.org/10.1128/JB.01122-06.
33. D'Elia MA, Millar KE, Beveridge TJ, Brown ED. 2006. Wall teichoic acid polymers are dispensable for cell viability in *Bacillus subtilis*. J Bacteriol 188:8313–8316. https://doi.org/10.1128/JB.01336-06.
34. Webb AJ, Karatsa-Dodgson M, Grundling A. 2009. Two-enzyme systems for glycolipid and polyglycerolphosphate lipoteichoic acid synthesis in *Listeria monocytogenes*. Mol Microbiol 74:299–314. https://doi.org/10.1111/j.1365-2958.2009.06829.x.
35. Das S, Kanamoto T, Ge X, Xu P, Unoki T, Munro CL, Kitten T. 2009. Contribution of lipoproteins and lipoprotein processing to endocarditis virulence in *Streptococcus sanguinis*. J Bacteriol 191:4166–4179. https://doi.org/10.1128/JB.01739-08.
36. Denham EL, Ward PN, Leigh JA. 2008. Lipoprotein signal peptides are processed by Lsp and Eep of *Streptococcus uberis*. J Bacteriol 190:4641–4647. https://doi.org/10.1128/JB.00287-08.
37. Vergara-Irigaray M, Maira-Litran T, Merino N, Pier GB, Penades JR, Lasa I. 2008. Wall teichoic acids are dispensable for anchoring the PNAG exopolysaccharide to the *Staphylococcus aureus* cell surface. Microbiology 154:865–877. https://doi.org/10.1099/mic.0.2007/013292-0.
38. Auchtung JM, Aleksanyan N, Bulku A, Berkmen MB. 2016. Biology of ICE*Bs1*, an integrative and conjugative element in *Bacillus subtilis*. Plasmid 86:14–25. https://doi.org/10.1016/j.plasmid.2016.07.001.
39. Dahmane N, Libante V, Charron-Bourgoin F, Guedon E, Guedon G, Leblond-Bourget N, Payot S. 2017. Diversity of integrative and conjugative elements of *Streptococcus salivarius* and their intra- and interspecies transfer. Appl Environ Microbiol 83:e00337-17. https://doi.org/10.1128/AEM.00337-17.
40. Bridier A, Dubois-Brissonnet F, Boubetra A, Thomas V, Briandet R. 2010. The biofilm architecture of sixty opportunistic pathogens deciphered using a high throughput CLSM method. J Microbiol Methods 82:64–70. https://doi.org/10.1016/j.mimet.2010.04.006.
41. Heydorn A, Nielsen AT, Hentzer M, Sternberg C, Givskov M, Ersboll BK, Molin S. 2000. Quantification of biofilm structures by the novel computer program COMSTAT. Microbiology 146:2395–2407. https://doi.org/10.1099/00221287-146-10-2395.
42. Sastalla I, Chim K, Cheung GY, Pomerantsev AP, Leppla SH. 2009. Codon-optimized fluorescent proteins designed for expression in low-GC gram-positive bacteria. Appl Environ Microbiol 75:2099–2110. https://doi.org/10.1128/AEM.02066-08.
43. Kebouchi M, Galia W, Genay M, Soligot C, Lecomte X, Awussi AA, Perrin C, Roux E, Dary-Mourot A, Le Roux Y. 2016. Implication of sortase-dependent proteins of *Streptococcus thermophilus* in adhesion to human intestinal epithelial cell lines and bile salt tolerance. Appl Microbiol Biotechnol 100:3667–3679. https://doi.org/10.1007/s00253-016-7322-1.
44. van de Guchte M, van der Vossen JM, Kok J, Venema G. 1989. Construction of a lactococcal expression vector: expression of hen egg white lysozyme in *Lactococcus lactis* subsp. *lactis*. Appl Environ Microbiol 55:224–228.
45. Maguin E, Prevost H, Ehrlich SD, Gruss A. 1996. Efficient insertional mutagenesis in lactococci and other gram-positive bacteria. J Bacteriol 178:931–935. https://doi.org/10.1128/jb.178.3.931-935.1996.
46. Takamatsu D, Osaki M, Sekizaki T. 2001. Thermosensitive suicide vectors for gene replacement in *Streptococcus suis*. Plasmid 46:140–148. https://doi.org/10.1006/plas.2001.1532.
47. Que YA, Haefliger JA, Francioli P, Moreillon P. 2000. Expression of *Staphylococcus aureus* clumping factor A in *Lactococcus lactis* subsp. *cremoris* using a new shuttle vector. Infect Immun 68:3516–3522. https://doi.org/10.1128/IAI.68.6.3516-3522.2000.